



Article

Unidirectional Ring-Based WDM Fiber Network for Both Downlink and Uplink Signal Access

Chien-Hung Yeh ^{1,*}, Wen-Piao Lin ², Yu-Ting Lai ¹, Lan-Yin Chen ¹, Chun-Yen Lin ¹, Kuan-Ming Cheng ¹, Teng-Yao Yang ¹ and Chi-Wai Chow ³

¹ Department of Photonics, Feng Chia University, Taichung 407802, Taiwan

² Department of Photonics, National Yang Ming Chiao Tung University, Hsinchu 300093, Taiwan; wplin@mail.cgu.edu.tw

³ Department of Electrical Engineering, Chang Gung University, Taoyuan 333323, Taiwan

* Correspondence: yehch@fcu.edu.tw

Abstract: In the paper, a dual-bidirectional ring-type wavelength-division-multiplexing (WDM) access network with downlink and uplink signal access simultaneously using a single fiber backbone in clockwise and counterclockwise directions, respectively. The proposed network architecture is simple and easy to implement via the designed remote node (RN) and optical line termination (OLT) modules, but it also can double the downlink traffic using the original WDM downlink wavelengths. The presented ring-type WDM network can also avoid the Rayleigh backscattering (RB) beat noise when the same wavelengths are applied as downlink and uplink channels concurrently. In the measurement, 50 km long-reach and 15 km short-reach fiber transmission lengths are achieved for the symmetrical 10 and 28 Gbit/s on-off keying (OOK) data access, respectively. In addition, based on the obtained power budgets of eight downlink WDM signals and network design at the forward error correction (FEC) threshold, 16 optical network units (ONUs) can be supported simultaneously.

Keywords: forward error correction (FEC); long-reach; ring-topology; Rayleigh backscattering (RB); WDM-PON



Citation: Yeh, C.-H.; Lin, W.-P.; Lai, Y.-T.; Chen, L.-Y.; Lin, C.-Y.; Cheng, K.-M.; Yang, T.-Y.; Chow, C.-W. Unidirectional Ring-Based WDM Fiber Network for Both Downlink and Uplink Signal Access. *Electronics* **2023**, *12*, 4264. <https://doi.org/10.3390/electronics12204264>

Academic Editors: Nakkeeran Kaliyaperumal and Suoda Chu

Received: 22 September 2023

Revised: 11 October 2023

Accepted: 13 October 2023

Published: 15 October 2023



Copyright: © 2023 by the authors. Licensee MDPI, Basel, Switzerland. This article is an open access article distributed under the terms and conditions of the Creative Commons Attribution (CC BY) license (<https://creativecommons.org/licenses/by/4.0/>).

1. Introduction

To satisfy the broadband capacity demand growth due to the wide applications of quantum networking, cloud computing, artificial intelligence (AI), internet traffic, data centers, big data, and 4K/8K video service, the access technology of fiber networks would be the best choice for data connection for the end-user [1–3]. Recently, optical access technologies include time-division-multiplexing (TDM) and wavelength-division-multiplexing passive optical networks (WDM-PONs) for high-speed and broad-capacity connection [4–7]. The TDM-PON is a point-to-multipoint (PtMP) and capacity-sharing access network. The uplink traffic for TDM-PON goes through a scheme called time division multiplexing access (TDMA). When the uplink signals from the whole optical network unit (ONU) are combined through a $1 \times N$ optical splitter (OSP), the TDMA transmission is applied to avoid signal collisions. For the downlink transmission, the data and corresponding information signal from the optical line termination (OLT) are delivered to corresponding ONUs and are multiplexed by applying a distinguished frame in the time domain for access. As we know, the first TSM-PON standard was defined in the 1980s [8]. Moreover, several TDM-PONs were proposed and studied in the 1990s to accomplish the target of fiber to the home (FTTH) [9]. The progress of TDM-PON is from 622.08 Mbit/s Broadband-PON (B-PON, in 2001) [10], 2.5 Gbit/s Gigabit-PON (G-PON, in 2008) [11], 10 Gb-capable PON (XG-PON, in 2012) [12] to 10 Gb-capable symmetric PON (XGS-PON, in 2016) [13] in ITU-T standards. Hence, the downlink traffic rate of the TDM system will be limited for each end-user due to the optical broadcasting and power-sharing [14]. To support higher TDM access rate, time and wavelength division multiplexing (TWDM)-PONs have been studied

to extend the downlink capacity to 40 Gbit/s by using four 10 Gbit/s WDM channels for next-generation PON Stage 2 (NG-PON2) [15,16]. The disadvantage of the TWDM-PON is that an adjustable filter or an adjustable laser light source needs to be added to the ONU. In general, the TWDM-PON also can provide a symmetrical 40 Gbit/s traffic rate for end users. However, once the number of users increases, the receiving downlink capacity of the user will also be reduced.

To provide and maintain enough data capacity of >1.25 Gbit/s to each subscriber and also deliver data information security, the WDM-PON system with a point-to-point (PtP) link can be implemented completely [17]. Although WDM-PON requires multiple WDM laser light sources and WDM MUX, it will increase the deployment and operating costs. However, WDM-PON's high-capacity transmission and signal security are worthy of being used in the future cloud and AI application industries. To reduce the cost and enhance the elasticity and reliability in WDM-PONs, the colorless ONUs have also been demonstrated when the Fabry–Perot laser diode (FP-LD), reflected semiconductor optical amplifier (RSOA) and wavelength-shift modulation method could be added for uplink signal remodulation [18–20]. The advantage of colorless ONU is that it can operate as an uplink signal without requiring an output wavelength of LD corresponding to the OLT and is easy to accomplish. Furthermore, the most common PON architecture is based on tree, ring, and hybrid topologies to be deployed according to the actual environment and requirements [20–22].

Once the same wavelengths are used as the downlink and uplink channels in tree-type WDM-PON networks for data traffic, the Rayleigh backscattering (RB) beat noise would be induced to influence the signal performance [23]. Moreover, as the fiber transmission length increases, the RB noise interference effect will also become greater. Thus, to prevent the RB noise in WDM-PON, researchers have studied the use of the electrical filtering method, Mach–Zehnder delay interferometer structure, phase-shift keying (DPSK) modulation skill, and optical carrier-suppressed subcarrier-modulation (OCS-SCM) technique [24–27].

In this paper, we design a bidirectional ring-based WDM-PON network for the downlink and uplink signal link simultaneously in clockwise and counterclockwise directions through a single fiber link, respectively. To reach the symmetric WDM signal transmission in the proposed fiber ring path, a new remote node (RN) module needs to be designed. In addition, the optical line terminal (OLT) also needs to make some changes to support dual-bidirectional fiber ring transmission for clockwise and counterclockwise links. According to the newly designed OLT and RN modules, we can completely avoid RB beat noise despite using the same WDM wavelength for downlink and uplink traffic on the same fiber path. Based on the designed ring-based fiber access network, each downlink wavelength can also be utilized to support two ONUs for doubling downlink traffic capacity. Then, in the demonstration, two corresponding experiment setups are proposed to demonstrate the long-reach and short-reach fiber transmissions, respectively, under various modulation data capacities. We use two sets of eight selected WDM wavelengths with 0.8 nm channel spacing (1535.82 to 1541.35 nm and 1542.14 to 1547.72 nm) acting as the downlink and uplink signals to verify the signal performance of 10 and 28 Gbit/s data rate, respectively. Here, the WDM downlink wavelengths of the OLT could support the double number of ONUs based on the designed ring-type PON system to achieve 50 km long-reach 10 Gbit/s and 15 km short-reach 28 Gbit/s on-off keying (OOK) data access without using fiber dispersion compensation, respectively. Thus, the presented WDM network can also provide symmetrical downlink and uplink access rates. As mentioned above, to avoid the fiber dispersion effect of 28 Gbit/s signal traffic, the fiber link length is set to 15 km for short-reach connection. This also means that we can use shorter or longer fiber transmission lengths at higher or lower transmission rates, respectively, according to the practical requirement. Furthermore, the obtained power sensitivities of the entire WDM downlink and uplink channels are from -27 to -25.5 dBm and -22.5 to -22.0 dBm at the symmetric 10 and 28 Gbit/s OOK modulation signal under the forward error correction (FEC) limit, which means the bit error rate (BER) is lower than 3.8×10^{-3} ,

after 50 and 15 km fiber links, respectively. Therefore, based on the obtained power budgets after long-reach and short-reach fiber connections, the proposed ring WDM-PON system can offer 16 ONUs by using the same eight downlink channels according to the obtained power budgets of the entire downlink and uplink wavelengths used.

2. Proposed Fiber Network Architecture

Figure 1 presents the proposed dual-bidirectional ring-type WDM-PON architecture for both downlink and uplink signal traffic through a single fiber backbone in clockwise and counterclockwise directions, respectively. The ring-based WDM network mainly consisted of an optical line terminal (OLT), remote node (RN), and optical network unit (ONU). In an OLT, the WDM signals are implemented as downlink traffic through different laser diodes (LDs) with corresponding wavelengths. As illustrated in Figure 1, each downlink WDM wavelength will be split into two channels (λ_n and λ'_n , where $n = 1, 2, 3, \dots$) through a 1×2 optical coupler (CP) and connect to the matching polarization controller (PC) and Mach-Zehnder modulator (MZM), respectively. Then, each WDM wavelength is split into two channels, which are connected to a 3-port optical circulator (OC) and then into a $1 \times N$ WDM multiplexer (Mux) for the counterclockwise ($\lambda_1, \lambda_2, \lambda_3, \dots, \text{ and } \lambda_n$) and clockwise transmission ($\lambda'_1, \lambda'_2, \lambda'_3, \dots, \text{ and } \lambda'_n$), simultaneously. In this design, we can apply two modulation rates of 10 and 28 Gbit/s formats on the corresponding MZM to realize the signal performances of the proposed ring-based WDM-PON, depending on the fiber length of 50 and 15 km. As seen in Figure 1, the WDM downlink signals of $\lambda_1, \lambda_2, \lambda_3, \dots, \text{ and } \lambda_n$ and $\lambda'_1, \lambda'_2, \lambda'_3, \dots, \text{ and } \lambda'_n$ will transmit through the connected ports “a” to “b” and “b” to “a” in counterclockwise and clockwise, respectively. Two split sets of downlink wavelengths will pass through each matching RN and be dropped into the corresponding two ONUs for data access. Hence, to deliver and assign the two split downlink signals to each corresponding ONU, the new RN module needs to be designed for operation.

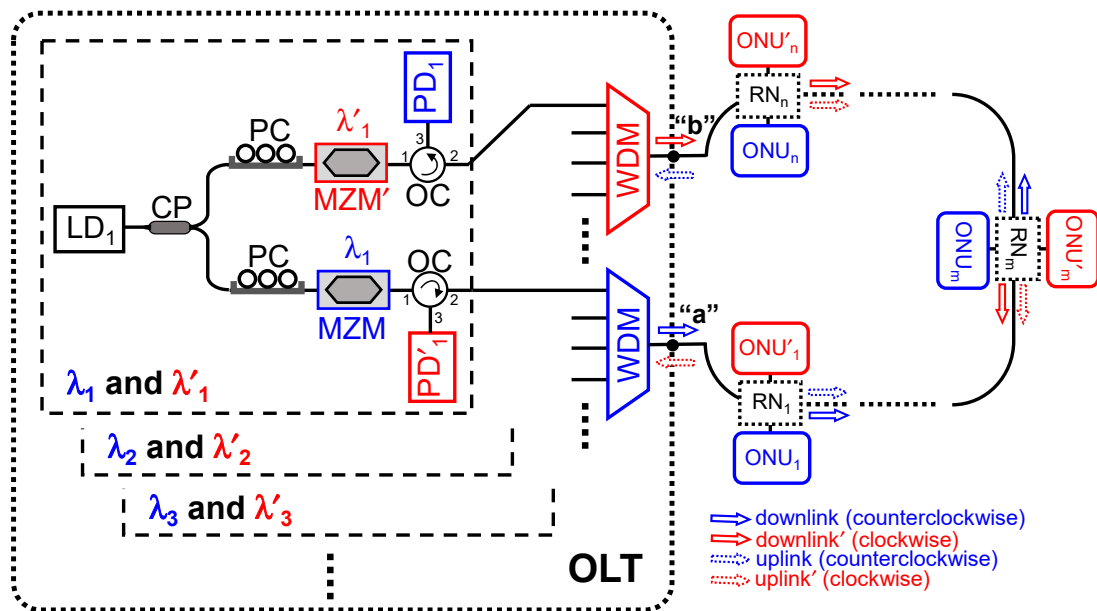


Figure 1. Proposed dual unidirectional ring-based WDM access architecture.

In the demonstration, the RN is comprised of six 3-port optical circulators (OC_1), two 4-port optical circulators (OC_2), and two corresponding fiber Bragg gratings (FBG_n and FBG'_n) with the same Bragg wavelength (λ_n and λ'_n) to add or drop the WDM signal, respectively, as exhibited in Figure 2a. The points “2” and “3” of OC_2 are used to receive and transmit corresponding downlink and uplink signals of ONU_n (or ONU'_n), respectively. When the downlink WDM wavelengths of $\lambda_1, \lambda_2, \lambda_3, \dots, \text{ and } \lambda_n$ (or $\lambda'_1, \lambda'_2, \lambda'_3, \dots, \text{ and } \lambda'_n$) from the OLT after passing through the RN, the corresponding WDM channel can

be dropped by the FBG_n (or FBG'_n) and enters the ONU_n (or ONU'_n). Moreover, the same uplink wavelength from the ONU_n (or ONU'_n) can also be reflected back to the OLT through the FBG_n (or FBG'_n) of the RN, as seen in Figure 2a. Thus, all the uplink signals of $\lambda_1, \lambda_2, \lambda_3, \dots,$ and λ_n (or $\lambda'_1, \lambda'_2, \lambda'_3, \dots,$ and λ'_n) will be transmitted through the same downlink fiber path in counterclockwise (or clockwise) transmission, as also illustrated in Figure 1. Then, the entire WDM uplink signals will be divided through the WDM Mux and received by the proper bandwidth photodiode (PD) of the OLT. In addition, the ONU_n consists of a corresponding LD_n , a PC, an MZM, and a PD to deliver and detect the uplink and downlink signal, respectively, as seen in Figure 2b. Therefore, as seen in Figures 1 and 2, each WDM downlink wavelength of the OLT can support two ONUs simultaneously via the RN through the same ring-based fiber path to improve wavelength usage efficiency. Regardless of whether it is a downlink or uplink signal, the insertion loss caused by passing through the RN is the same. Additionally, the demonstrated WDM access system can also enable symmetrical downlink and uplink traffic rates.

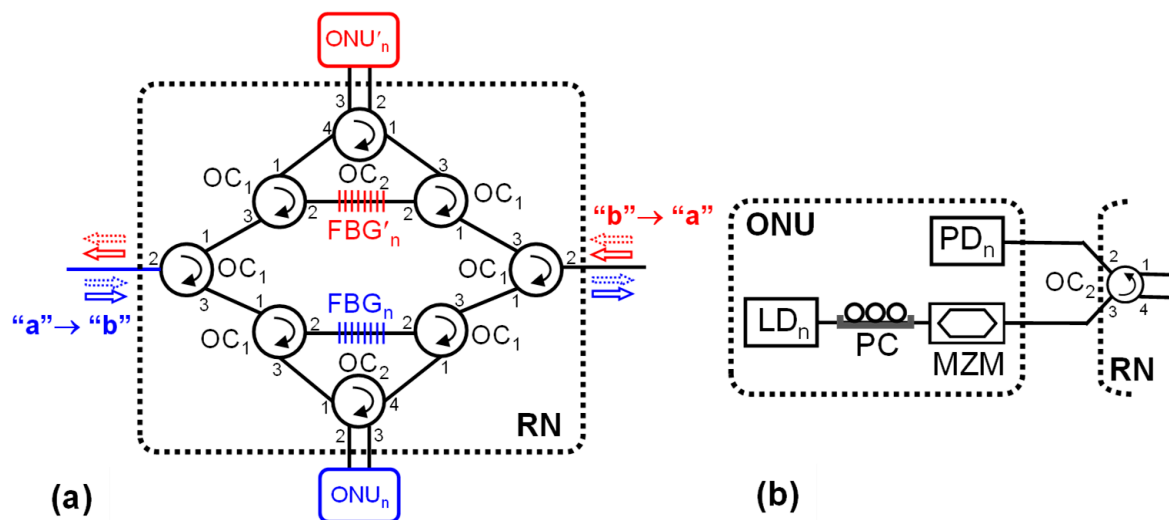


Figure 2. (a) New designed RN module and (b) the construction of each ONU.

3. Experiment and Results

To enforce the symmetrical signal performance of the presented ring-based WDM PON network, the experimental setups of downlink and uplink transmission are built for proof of concept, respectively, as shown in Figure 3a,b. A tunable laser source (TLS) is applied as the optical transmitter (Tx) for downlink or uplink transmissions to demonstrate different WDM wavelength outputs. In the first measurement of long-reach signal transmission, the TLS is used to connect to the PC, 10 GHz MZM, a 50 km single-mode fiber (SMF), three OCs, an FBG, a variable optical attenuator (VOA), an erbium-doped fiber amplifier (EDFA), and a 10 GHz PIN PD for downlink traffic, as shown in Figure 3a. The three OCs and FBGs in Figure 3a are used to conduct signal transmission experiments corresponding to the RN in Figure 2a. The PC is adjusted suitably to maintain and achieve the optimal optical output power. The VOA and EDFA are used to act as the optical pre-amplifier to enhance the detected power sensitivity of the downlink signal. We apply 10 Gbit/s on-off keying (OOK) format with a pattern length of $2^{15} - 1$ on MZM to generate a downlink modulation signal. In addition, the corresponding experimental setup of uplink transmission is also plotted in Figure 3b. The transmission experiment in Figure 3b also corresponds to the designed architecture in Figure 2a. The uplink modulation rate and fiber transmission length are also set to 10 Gbit/s and 50 km long. As mentioned above, the symmetrical 10 Gbit/s downlink and uplink rates can be executed and performed in the demonstration.

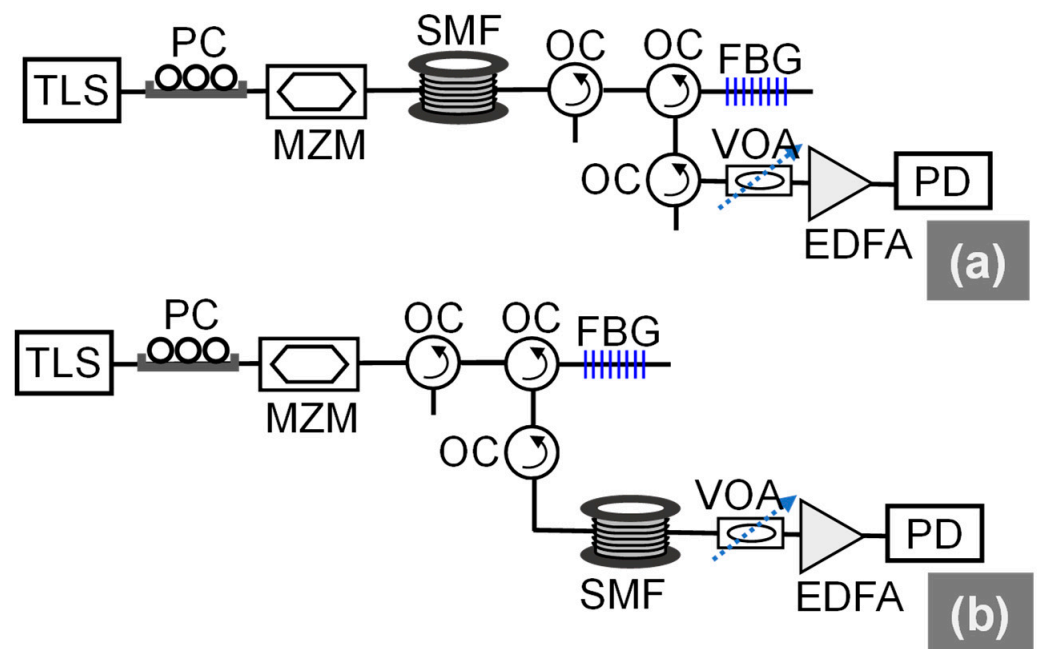


Figure 3. Experimental setup of the BER measurements for (a) downlink and (b) uplink transmission, respectively.

In the experiment, eight WDM wavelengths of 1538.82, 1536.61, 1537.40, 1538.19, 1538.98, 1539.77, 1540.56, and 1541.35 nm are employed for the symmetrical downlink and uplink traffic, respectively. The channel spacing of the eight wavelengths used is around 0.8 nm to avoid the channel cross-talk effect. And the SMF type used for signal transmission in the experiment is ITU-T Recommendation G.652. Figure 4a,b exhibits the measured bit error rate (BER) behaviors of 10 Gbit/s OOK downlink and uplink WDM signals at the back-to-back (BtB) state and after 50 km SMF transmission, respectively. The obtained power sensitivities of eight WDM signals are in the ranges of -27 to -25 dBm and -27 to -25.5 dBm at the BtB and through the 50 km SMF link, respectively, within the forward error correction (FEC) limit, which means the $BER \leq 3.8 \times 10^{-3}$. The above results show that there is almost no optical power penalty under 50 km fiber transmission. In fact, the fiber dispersion effect would result in an optical power penalty after passing through the fiber link length. The longer fiber transmission distance will cause the power penalty to become larger. It should be noted that in this experiment, we use the 10 GHz MZM with a -0.7 chirp parameter to modulate and transmit 10 Gbit/s OOK signals. The negative chirp of MZM can pre-compensate fiber dispersion after 50 km long-reach SMF transmission. Thus, there is no power penalty observed, and the measured sensitivities at the BtB status and after 50 km fiber link are almost the same, respectively, as shown in Figures 4a and 4b. Here, the achievable power sensitivity at each wavelength can be used to estimate the corresponding power budget to confirm that the total insertion loss can be lower than that caused by the PON system. And we will explain this in more detail in the next section. The insets of Figure 4a,b are the measured corresponding eye diagrams of the eight wavelengths selected at the maximum optical received powers. All the observed eyes are open, clean, and identical. In this way, regardless of counterclockwise or clockwise transmissions, the total fiber distance of the ring link can reach 100 km long (50 km SMF downlink length + 50 km SMF uplink length).

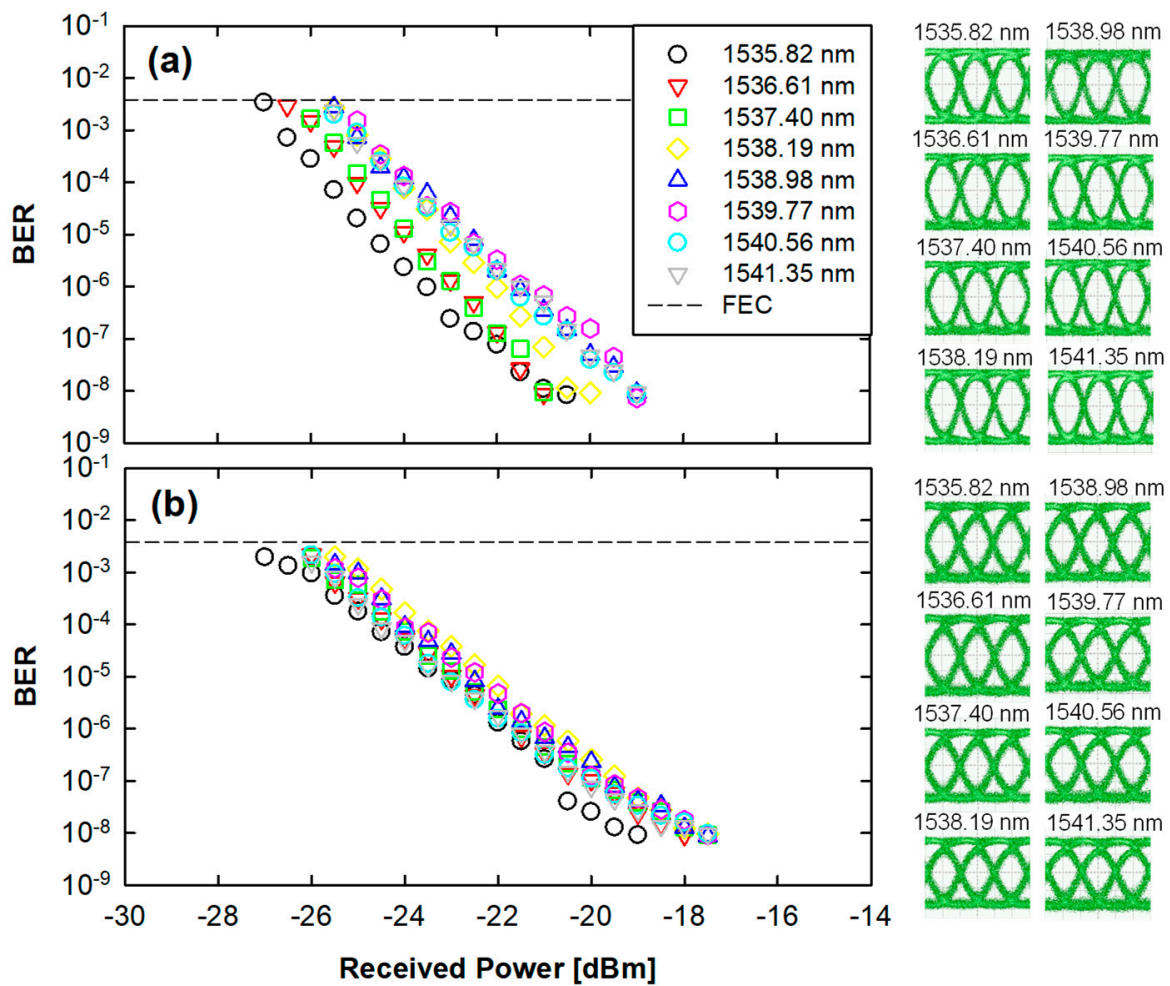


Figure 4. Measured bit error rate (BER) behaviors of 10 Gbit/s OOK WDM signals (a) at the BtB and (b) after 50 km SMF transmission, respectively. Insets are the measured eye diagrams of eight selected wavelengths at the BtB and 50 km SMF link, respectively.

In this section, we will analyze and discuss the total insertion loss and power budget induced by the proposed ring-based WDM-PON architecture if the output power of each WDM signal is set to 7.5 dBm at the point “a” or “b” of the OLT in Figure 1. Then, the obtained power budget can be achieved in a range of 33.0 [7.5 – (–25.5)] to 34.5 dB under the eight channels used after 50 km fiber link. Here, we assume that all the WDM downlink signals will initially go through the entire RNs and 50 km SMF transmission. As displayed in Figure 2a, each RN will induce a 2.5 dB insertion loss [link path: OC₁ (0.5 dB) → OC₁ (0.5 dB) → FBG_n (0.5 dB) → OC₁ (0.5 dB) → OC₁ (0.5 dB)], when the WDM downlink signals are not reflected by the corresponding FBG_n. If the corresponding downlink signal is reflected by the FBG_n and then into the ONU_n, it would also result in a 2.5 dB insertion loss [link path: OC₁ (0.5 dB) → OC₁ (0.5 dB) → FBG_n (0.5 dB) → OC₁ (0.5 dB) → OC₂ (0.5 dB)]. For uplink signal transmission, the resulting total insertion loss is the same as for the downlink signal, as illustrated in Figure 2a,b. Whether it is downlink or uplink signal transmission, the total insertion loss is the same. Hence, we can utilize the simple experimental setup of Figure 3a,b to represent the downlink and uplink traffic, respectively. Let us take the eight selected WDM wavelengths and the resulting power budget of 33 dB as an example. After passing through eight ONUs and 50 km SMF transmission length, the total induced insertion losses of downlink and uplink traffic would be 30 dB (2.5 dB × 8 ONUs + 0.2 dB × 50 km SMF). Finally, there will be 3 dB of remaining power budget in the measurement. As a result, we can achieve the symmetrical 10 Gbit/s OOK WDM downlink and uplink access after 50 km long-reach

SMF transmission simultaneously. Moreover, the eight RNs can support 16 ONUs based on using the eight selected WDM wavelengths and the same single fiber path.

In the second experiment, we also can perform the larger modulation rate of 28 Gbit/s OOK in the ring-based WDM-PON for a 15 km short-reach fiber link based on the same setup of Figure 3a,b. Then, we use the 40 GHz MZM with normal chirp and 40 GHz PIN PD instead of the 10 GHz device to generate 28 Gbit/s OOK WDM signal for observing BER performance. Due to the 28 Gbit/s data rate in the presented bidirectional ring-type PON without dispersion compensation, the SMF transmission length needs to be reduced to 15 km for the downlink and uplink connection to avoid the fiber dispersion issue. We select eight WDM wavelengths of 1542.14, 1542.94, 1543.73, 1544.53, 1545.32, 1546.12, 1546.92, and 1547.72 nm to represent the downlink and uplink signals for testing the BER performance, respectively. Here, the modulation pattern length of $2^{15} - 1$ is formatted on the 40 GHz MZM to reach the symmetrical downlink and uplink transmissions. Figure 5a,b exhibits the corresponding BER output of the eight selected WDM wavelengths at the BtB state and through the 15 km SMF transmission distance without dispersion compensation, respectively. The detected power sensitivities of the eight wavelengths are in the range of -23.0 to -22.5 dBm and -22.5 to -22.0 dBm at the BtB and after 15 km fiber link under the FEC target ($\text{BER} \leq 3.8 \times 10^{-3}$), respectively. The power penalty span of 0.5 to 1 dB is caused due to the 15 km SMF connection. The insets of Figure 5a,b are the observed eye diagrams of the eight wavelengths at the maximum received powers. All the received eye diagrams are also open and clean at the BtB and after 15 km fiber link, respectively. Since the fiber dispersion effect will affect the 28 Gbit/s OOK capacity through 15 km SMF transmission, its optical sensitivity will be smaller than that of 10 Gbit/s OOK modulation. Thus, the corresponding power budget of 29.5 [7.5 – (–22)] to 30 dB [7.5 – (–22.5)] is achieved after 15 km fiber transmission, while 7.5 dBm output powers of downlink and uplink signals are also applied. The downlink and uplink WDM wavelengths will induce the same insertion loss of 23 dB [$2.5 \text{ dB} \times 8$ (ONUs) + $0.2 \text{ dB} \times 15$ (km SMF)] after passing through 8 ONUs. In the demonstration, the smallest power budget of 29.5 dB can also meet with the total insertion loss of 23 dB induced by the presented WDM access network. We still have a ~ 6.5 dB redundant power budget in the 28 Gbit/s traffic case when eight RNs are added to the ring network architecture. This means that the 28 Gbit/s data transmission system may be able to add some more fiber transmission length or add another RN. As a result, no matter the long-reach or short-reach fiber link with low capacity and high data capacity, the proposed ring-type WDM-PON architecture can provide twice ONU numbers for signal access based on the original downlink wavelengths and avoid the RB beat noise.

Table 1a,b presents the measured parameter of output performance in the proposed ring-type WDM-PON architecture when the modulation rate is set at 10 and 25 Gbit/s OOK format through the 50 and 10 km SMF transmission, respectively. To achieve a longer fiber transmission length in 10 Gbit/s OOK modulation, a -0.7 chirp parameter 10 GHz MZM is employed to cause the dispersion pre-compensation effect. However, the 40 GHz MZM is experimented with using a common chirp parameter. Due to the fiber dispersion effect, 28 Gbit/s OOK modulation is used for transmission only through a 15 km fiber connection for demonstration. The obtained power sensitivities are -27 to -25.5 dBm and -22.5 to -22 dBm at the 10 and 28 Gbit/s OOK modulations after 50 and 15 km fiber connection lengths, respectively. Although the access system experiments are conducted under different signal modulation rates and fiber transmission distances, the power budget obtained by the two measurements can support eight RNs. As seen in Table 1, whether under 10 Gbit/s or 28 Gbit/s traffic data transmission, 16 ONUs can be supported simultaneously according to the resulting power budget without the use of EDFA in the fiber ring architecture.

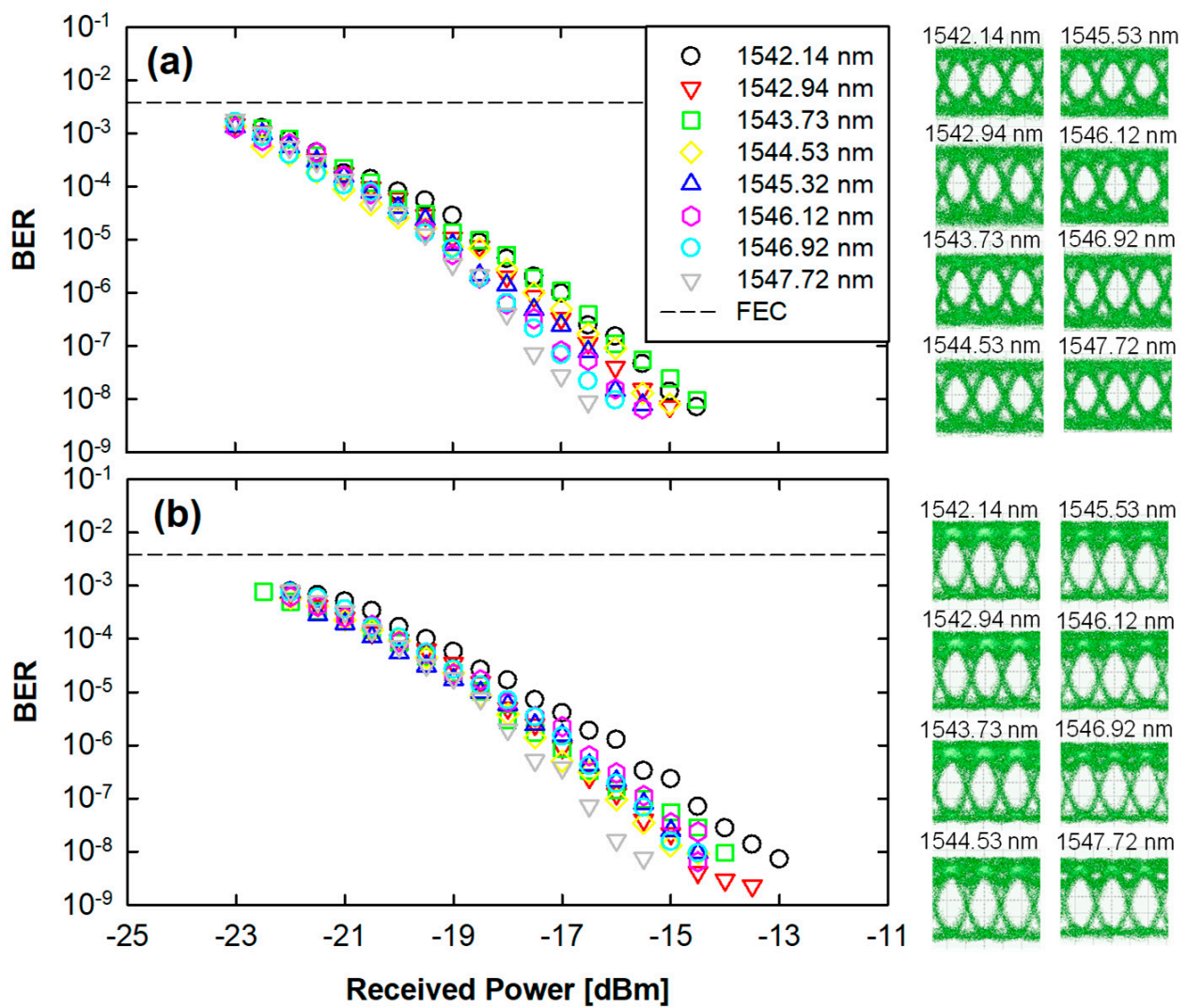


Figure 5. Measured bit error rate (BER) behaviors of 28 Gbit/s OOK WDM signals (a) at the BtB and (b) after 15 km SMF transmission, respectively. Insets are the measured eye diagrams at the wavelength of 1542.14 nm. Insets are the measured eye diagrams of eight selected wavelengths at the BtB and 15 km SMF link, respectively.

Table 1. Measured parameter of output performance in the proposed ring-type WDM-PON architecture at (a) 10 and (b) 28 Gbit/s OOK format through 50 and 10 km SMF transmission, respectively.

(a) 10 Gbit/s OOK	1535.82 nm	1536.61 nm	1537.40 nm	1538.19 nm	1538.98 nm	1539.77 nm	1540.56 nm	1541.35 nm
Input Power (dBm)	7.5	7.5	7.5	7.5	7.5	7.5	7.5	7.5
Sensitivity (dBm)	−27	−26.5	−26	−25.5	−25.5	−25	−25	−25
BER (BtB)	3.39×10^{-3}	2.91×10^{-3}	1.68×10^{-3}	2.64×10^{-3}	2.77×10^{-3}	1.53×10^{-3}	1.93×10^{-3}	2.4×10^{-3}
Sensitivity (dBm)	−27	−26	−26	−25.5	−25.5	−25.5	−26	−26
BER (50 km)	1.94×10^{-3}	2.18×10^{-3}	1.89×10^{-3}	1.97×10^{-3}	1.43×10^{-3}	1.19×10^{-3}	2.14×10^{-3}	1.57×10^{-3}
Power Budget (dB)	34.5	33.5	33.5	33	33	33	33.5	33.5
(b) 28 Gbit/s OOK	1542.14 nm	1542.94 nm	1543.73 nm	1544.53 nm	1545.32 nm	1546.12 nm	1547.72 nm	1548.51 nm
Input Power (dBm)	7.5	7.5	7.5	7.5	7.5	7.5	7.5	7.5
Sensitivity (dBm)	−22.5	−23	−23	−23	−23	−23	−23	−23.5
BER (BtB)	1.26×10^{-3}	1.48×10^{-3}	1.50×10^{-3}	1.32×10^{-3}	1.33×10^{-3}	1.28×10^{-3}	1.65×10^{-3}	1.79×10^{-3}
Sensitivity (dBm)	−22	−22	−22.5	−22	−22	−22	−22	−22
BER (15 km)	7.71×10^{-4}	7.43×10^{-4}	7.71×10^{-4}	5.88×10^{-4}	7.52×10^{-4}	6.26×10^{-4}	7.50×10^{-4}	7.93×10^{-4}
Power Budget (dB)	29.5	29.5	30	29.5	29.5	29.5	29.5	29.5

4. Conclusions

We proposed a dual-bidirectional ring-based WDM-PON architecture with symmetrical downlink and uplink connection simultaneously in clockwise and counterclockwise directions through the same single fiber backbone. In this ring network, the WDM downlink and uplink traffic were transmitted on the single fiber path with the same direction based on the newly designed OLT and RN modules. Thus, the RB beat noise could also be prevented when the same WDM signals were used. Furthermore, the original WDM downlink wavelengths of the OLT could support the double number of ONUs through the designed ring-type PON to achieve 50 km long-reach 10 Gbit/s OOK or 15 km short-reach 28 Gbit/s OOK signal access. In the measurement, when eight same WDM wavelengths were employed simultaneously to regard as the downlink and uplink channels, the detected power sensitivities were in the range of -27 to -26 dBm and -22.5 to -22.0 dBm at the symmetrical 10 and 28 Gbit/s OOK signal under the FEC limit ($\text{BER} \leq 3.8 \times 10^{-3}$) after 50 and 15 km fiber links, respectively. According to the obtained power budgets of 10 Gbit/s long-reach or 28 Gbit/s short-reach transmissions through a single ring fiber, the proposed WDM-PON could support 16 ONUs by utilizing eight WDM downlink channels. As a result, based on the designed ring-type WDM-PON architecture, the original downlink channel numbers could double the ONU numbers in last-mile access and avoid the RB interferometric beat noise.

Author Contributions: Data curation, Y.-T.L., L.-Y.C., C.-Y.L., K.-M.C. and T.-Y.Y.; Execution, Y.-T.L., L.-Y.C., C.-Y.L., K.-M.C. and T.-Y.Y.; Investigation, C.-H.Y.; Supervision, W.-P.L. and C.-W.C.; Writing—review and editing, C.-H.Y. All authors have read and agreed to the published version of the manuscript.

Funding: National Science and Technology Council (NSTC), Taiwan, NSTC-110-2221-E-035-058-MY2 and NSTC-112-2221-E-035-059-MY3; Chang Gung University, Taiwan, BMRP-740.

Data Availability Statement: The data presented in this study are available on request from the corresponding author. The data are not publicly available due to privacy restrictions.

Conflicts of Interest: The authors declare no conflict of interest.

References

- Houtsma, V.; Mahadevan, A.; Kaneda, N.; Veen, D.V. Transceiver technologies for passive optical networks: Past, present, and future. *J. Opt. Commun. Netw.* **2021**, *13*, A44–A55. [[CrossRef](#)]
- Lin, G.-R.; Wang, H.-L.; Lin, G.-C.; Huang, Y.-H.; Lin, Y.-H.; Cheng, T.-K. Comparison on injection-locked Fabry-Perot laser diode with front-facet reflectivity of 1% and 30% for optical data transmission in WDM-PON system. *J. Lightw. Technol.* **2009**, *27*, 2779–2785.
- Cheng, N.; Gao, J.; Xu, C.; Gao, B.; Liu, D.; Wang, L.; Wu, X.; Zhou, X.; Lin, H.; Effenberger, F. Flexible TWDM PON system with pluggable optical transceiver modules. *Opt. Express* **2014**, *22*, 2078–2091. [[CrossRef](#)] [[PubMed](#)]
- Kumari, M.; Sharma, R.; Sheetal, A. Performance analysis of high speed backward compatible TWDM-PON with hybrid WDM-OCDMA PON using different OCDMA codes. *Opt. Quantum Electron.* **2020**, *52*, 482. [[CrossRef](#)]
- Yeh, C.-H.; Liu, L.-H.; Lin, W.-P.; Ko, H.-S.; Lai, Y.-T.; Chow, C.-W. A survivable optical network for WDM access against fiber breakpoint. *IEEE Access* **2022**, *10*, 25828–25833. [[CrossRef](#)]
- Lin, G.-R.; Liao, Y.-S.; Chi, Y.-C.; Kuo, H.-C.; Lin, G.-C.; Wang, H.-L.; Chen, Y.-J. Long-cavity Fabry-Perot laser amplifier transmitter with enhanced injection-locking bandwidth for WDM-PON application. *J. Lightw. Technol.* **2010**, *28*, 2925–2932. [[CrossRef](#)]
- Alharbi, A.G.; Singh, M. Downstream performance evaluation of a 4×112 Gbps hybrid wavelength-polarization division multiplexed next generation-passive optical network. *Opt. Quantum Electron.* **2022**, *54*, 384. [[CrossRef](#)]
- Stern, J.R.; Balance, J.W.; Faulkner, D.W.; Hornung, S.; Payne, D.B.; Oakely, K. Passive optical local networks for telephony applications and beyond. *Electron. Lett.* **1987**, *23*, 1255–1256. [[CrossRef](#)]
- Kumozaki, K. Optical access systems: Present state and future directions. *NTT Tech. Rev.* **2008**, *6*, 1–7.
- ITU-T Recommendation G.983 Series: Broadband Passive Optical Network; International Telecommunication Union (ITU): Geneva, Switzerland, 2001.
- ITU-T Recommendation G.984 Series: Gigabit Capable Passive Optical Network (G-PON); International Telecommunication Union (ITU): Geneva, Switzerland, 2008.
- ITU-T Recommendation G.987 Series: 10 Gigabit-Capable Passive Optical Network (XG-PON); International Telecommunication Union (ITU): Geneva, Switzerland, 2012.

13. ITU-T Recommendation G.9807 Series: 10 Gigabit Capable Symmetric Passive Optical Network (XGSPON); International Telecommunication Union (ITU): Geneva, Switzerland, 2016.
14. Mikaeil, A.M.; Hu, W.; Ye, T.; Hussain, S.B. Performance evaluation of XG-PON based mobile front-haul transport in cloud-RAN architecture. *J. Opt. Commun. Netw.* **2017**, *9*, 984–994. [[CrossRef](#)]
15. Luo, Y.; Zhou, X.; Effenberger, F.; Yan, X.; Peng, G.; Qian, Y.; Ma, Y. Time- and wavelength-division multiplexed passive optical network (TWDM-PON) for next-generation PON stage 2 (NG-PON2). *J. Light. Technol.* **2013**, *31*, 587–593. [[CrossRef](#)]
16. Yeh, C.H.; Chow, C.W.; Yang, M.H.; Hsu, D.Z. A flexible and reliable 40 Gb/s OFDM downstream TWDM-PON architecture. *IEEE Photon. J.* **2015**, *7*, 7905709. [[CrossRef](#)]
17. Kodama, T.; Matsumoto, R.; Inoue, T.; Namiki, S.; Jinno, M. Baud-rate-adaptive OLT integrated-coherent transceiver for Nyquist spectral shaped/channel spaced WDM-PON. In Proceedings of the Opto-Electronics and Communications Conference (OECC) 2020, Taipei, Taiwan, 4–8 October 2020; pp. 1–3.
18. Deng, M.L.; Giddings, R.P.; Tsai, C.-T.; Lin, G.-R.; Tang, J.M. Colorless WRC-FPLDs subject to gain-saturated RSOA feedback for WDM-PONs. *IEEE Photon. Technol. Lett.* **2018**, *30*, 43–46. [[CrossRef](#)]
19. Yeh, C.H.; Chow, C.W.; Huang, S.P.; Sung, J.Y.; Liu, Y.L.; Pan, C.L. Ring-based WDM access network providing both Rayleigh backscattering noise mitigation and fiber-fault protection. *J. Lightw. Technol.* **2012**, *30*, 3211–3218. [[CrossRef](#)]
20. Yao, H.; Li, W.; Feng, Q.; Han, J.; Ye, Z.; Hu, Q.; Yang, Q.; Yu, S. Ring-based colorless WDM-PON with Rayleigh backscattering noise mitigation. *J. Opt. Commun. Netw.* **2017**, *9*, 27–35. [[CrossRef](#)]
21. Kodama, T.; Azuma, Y.; Ishikawa, T. Colorless and directionless coherent WDM-PON architecture with extended star topology using a self-healing for bidirectional link protection. In Proceedings of the Opto-Electronics and Communications Conference (OECC) 2020, Taipei, Taiwan, 4–8 October 2020; pp. 1–3.
22. Sun, X.; Wang, Z.; Chan, C.-K.; Chen, L.-K. A novel star-ring protection architecture scheme for WDM passive optical access networks. In Proceedings of the Optical Fiber Communication Conference (OFC) 2005, Anaheim, CA, USA, 6–11 March 2005; p. JWA53.
23. Hong, U.H.; Cho, K.Y.; Takushima, Y.; Chung, Y.C. Effects of Rayleigh backscattering in long-reach RSOA-based WDM PON. In Proceedings of the Optical Fiber Communication Conference (OFC) 2010, San Diego, CA, USA, 21–25 March 2010; p. OThG1.
24. Choudhury, P.K. Analysis of post detection ad-hoc filter based loopback WDM-PONs to enhance the tolerance against Rayleigh backscattering noise. In Proceedings of the International Conference on Electrical and Computer Engineering 2012, Dhaka, Bangladesh, 20–22 December 2012; pp. 47–50.
25. Yeh, C.-H.; Ko, H.-S.; Liaw, S.-K.; Liu, L.-H.; Chen, J.-H.; Chow, C.-W. A survivable and flexible WDM access network by alternate FSO- and fiber-paths for fault protection. *IEEE Photon. J.* **2022**, *14*, 7209205. [[CrossRef](#)]
26. Xu, J.; Li, M.; Chen, L.-K. Rayleigh noise reduction in 10-Gb/s carrier-distributed WDM-PONs using in-band optical filtering. *J. Lightw. Technol.* **2011**, *29*, 3632–3639.
27. Chowdhury, A.; Chien, H.-C.; Huang, M.-F.; Yu, J.; Chang, G.-K. Rayleigh backscattering noise-eliminated 115-km long-reach bidirectional centralized WDM-PON with 10-Gb/s DPSK downstream and remodulated 2.5-Gb/s OCS-SCM upstream signal. *IEEE Photon. Technol. Lett.* **2008**, *20*, 2081–22083. [[CrossRef](#)]

Disclaimer/Publisher’s Note: The statements, opinions and data contained in all publications are solely those of the individual author(s) and contributor(s) and not of MDPI and/or the editor(s). MDPI and/or the editor(s) disclaim responsibility for any injury to people or property resulting from any ideas, methods, instructions or products referred to in the content.